

Rosai-Dorfman Disease in a Pediatric Patient: Imaging Findings and Pathology with a brief review of the Literature

Thomas Hartmann, B.S.^{1*}, Nadia Solomon, MD, MSc, MA², Gabriel Lerner, MD, MS³, Lauren Ehrlich, MD²


¹Medical Student, University of Central Florida College of Medicine, Orlando, USA

²Department of Radiology and Biomedical Imaging, Yale New Haven Hospital, New Haven, USA

³Department of Pathology and Laboratory Medicine, Yale New Haven Hospital, New Haven, USA

⁴Department of Radiology and Biomedical Imaging, Yale New Haven Hospital, New Haven, USA

*Correspondence: Thomas Hartmann, B.S., University of Central Florida College of Medicine, 6850 Lake Nona Blvd, Orlando, FL 32827, USA

 tch5167@knights.ucf.edu

Radiology Case. 2023 Aug; 17(9):1-14 :: DOI: 10.3941/jrcr.v17i8.4873

ABSTRACT

Rosai-Dorfman Disease, otherwise known as sinus histiocytosis with massive lymphadenopathy, is a rare form of non-Langerhans cell histiocytosis with an estimated incidence of 100 cases per year in the United States. Due to its variable presentation and nonspecific clinical findings, it is particularly difficult to diagnose in pediatric patients. We report a case of an 11-month-old male who presented with a 4-day history of a right groin mass. Ultrasound of the groin and pelvis demonstrated, and MRI of the abdomen and pelvis confirmed an inguinal mass with surrounding lymphadenopathy. Pathology confirmed Rosai-Dorfman Disease and the patient improved after starting oral steroid therapy. To the best of our knowledge, this is the first case of Rosai-Dorfman Disease involving the inguinal region in an infant under 1 year of age reported in the literature. In this case report, we discuss the imaging and histology findings as well as provide a brief literature review for this diagnosis.

CASE REPORT

CASE REPORT

An 11-month-old male with no significant medical history was brought to the emergency department (ED) by his mother due to a right inguinal mass, first noticed four days prior. According to his mother, the patient had a low-grade fever (T_{\max} 100F) and congestion for the past week as well as increased irritability. He was otherwise eating, drinking, and urinating normally. His mother denied any drainage, noticeable discoloration, or significant changes in the size of the mass since initially noticing it. The patient was born vaginally at term, had reached age-appropriate milestones, and was up-to-date on his immunizations. His mother denied recent travel or sick contacts at home. Inquiry into family history for malignancies was unrevealing.

The patient's vital signs were within normal range, and he was afebrile in the ED. Although his mother endorsed changes in activity and a subjective fever, she denied constitutional symptoms including appetite change, diaphoresis, fatigue, or unexpected weight loss. Abdominal exam demonstrated a palpable, reducible mass in the right inguinal/groin region with no overlying discoloration or drainage. Testicles were

descended, intrascrotal, and normal in size bilaterally with no discoloration or tenderness. Initial differential diagnosis in the ED included infection, hernial abnormality, and testicular pathology with lesser concern for malignancy (i.e. lymphoma). Bedside ultrasound (US) along with blood tests were ordered for further evaluation.

Complete blood count showed an elevated white blood count ($14.2 \times 10^9/L$) and absolute neutrophil count ($10,800 \text{ cells}/\text{mm}^3$) without blasts. Patient's labs were consistent with iron deficiency anemia with a hemoglobin of $7.8\text{g}/\text{dL}$, MCV of 77.4fL , and iron of $20 \text{ mcg}/\text{dL}$. Other notable labs included an elevated erythrocyte sedimentation rate ($76 \text{ mm}/\text{h}$) and C-reactive protein ($79.5 \text{ mg}/\text{L}$). Patient's uric acid and lactate dehydrogenase levels were within normal limits. US examination with Doppler demonstrated a lobulated, soft tissue mass ($5.6 \times 3.3 \times 3.5\text{cm}$) extending into the right lower quadrant/hemipelvis with multiple enlarged lymph nodes (Figures 1,2). US evaluation of the groin revealed thickened right-sided paratesticular tissue but otherwise no sign of torsion or bowel-containing hernia. At this time, due to concern for malignancy, Hematology/Oncology was consulted and recommended admitting the patient to the hospital for further imaging with magnetic resonance imaging (MRI).

MRI with contrast demonstrated a necrotic lesion at the posterior right pelvic inlet measuring 4.3cm in diameter. Additional findings included enhancing, clustered right inguinal, external iliac, and common iliac lymphadenopathy (Figure 3). The MRI also revealed prominent, hyper-enhancing nodules in the interaortocaval region and left lateral chest wall concerning for potential metastatic foci (Figure 4,5). Interventional radiology was consulted to perform an US-guided biopsy of the mass (Figure 6).

Histopathologic evaluation revealed lymphoid tissue with sinus histiocytosis and focal acute inflammation. There was also a prominent population of histiocytes with large nuclei and voluminous cytoplasm showing emperipolesis with engulfed lymphocytes. Histiocytic population staining was positive for S100, OCT2 (nuclear) and Cyclin D1 (nuclear), and weakly positive for CD68 (cytoplasmic). Tissue was negative for CD1a (Figure 7). Overall, this constellation of findings is consistent with a diagnosis of Rosai-Dorfman Disease (RDD). Tumor profiling was significant for a *KRAS* mutation.

Per Hematology/Oncology recommendation, whole body PET-CT was ordered to evaluate for extent of disease prior to starting therapy. Findings in the head and neck region showed multiple hypermetabolic conglomerate nodes within the cervical, parotid, and supraclavicular areas — right greater than left. Two visualized nodes included a right supraclavicular mass with a standardized uptake value (SUV) max of 8.2 and a right level 5 conglomerate with an SUV max of 8. In the chest region, hypermetabolic foci were identified within the mediastinum and left axilla with SUV max of 4.9 and 2.8, respectively. Abdomen and pelvis region demonstrated a large ill-defined hypermetabolic conglomerate mass extending from the aortocaval region to the lower pelvis, predominately on the right side, with SUV max of 10. In addition, multiple hypermetabolic conglomerate nodes were visualized within the right inguinal region with SUV max of 8.2 (Figure 8).

The patient was discharged on a course of oral prednisone therapy (1mg/kg/day). On follow-up visit three weeks later, the mother reported interval decrease in the size of the patient's cervical and inguinal lymphadenopathy since starting therapy. She denied irritability, insomnia, bone pain, and any signs of gastritis. Computer tomography (CT) of the chest and MRI of the neck, abdomen, and pelvis were ordered to assess clinical response. MRI of the abdomen and pelvis demonstrated a decrease in the size of the dominant lesion at the right pelvic inlet measuring 2.0cm in greatest diameter versus 4.3cm on prior MRI. No significant changes in the surrounding clustered retroperitoneal and inguinal lymphadenopathy were identified (Figure 9). MRI of the neck showed a decrease in cervical lymphadenopathy when compared to prior whole-body PET/CT (Figure 10). CT chest was unchanged from prior PET/CT, again showing right paratracheal lymphadenopathy and similar size of the left chest wall nodule (Figure 11).

Four months post-initial presentation, patient was still on

a slow prednisone taper after completing a month-long steroid course (1mg/kg/day). Given an examination consistent with a continued positive response to steroid therapy, the decision was made to continue the prednisone taper. If worsening adenopathy or end-organ dysfunction were to become a concern, 2nd line therapy consisting of either an mTOR inhibitor or MAPK kinase (MEK) inhibitor based on patient's *KRAS* mutation was discussed as a future adjunct therapy.

Six months post-initial presentation, the patient arrived at the clinic having now completed the long steroid taper. On history and physical examination, he was currently asymptomatic with findings consistent with a partial clinical response. Based on published data on RDD, the treatment team decided on continuing with observation and monitoring for disease progression rather than starting any further systemic therapy.

DISCUSSION

Etiology & Demographics

RDD, otherwise known as sinus histiocytosis with massive lymphadenopathy, occurs due to an overproduction of histiocytes in the lymph nodes. It is a rare form of non-Langerhans cell histiocytosis with an estimated incidence of 100 cases per year in the United States [1]. The disease prevalence is higher in males than females (58% to 42%) with a mean age of onset of 20.6 years [2]. Due to its rarity, few cases of RDD have been reported in the pediatric community, specifically in infants. To the best of our knowledge, this is the first reported RDD case in an infant under 1 year of age involving the inguinal region.

Pathogenesis

The pathogenesis of RDD is not well-defined and likely inconsistent across the spectrum of RDD phenotypes; however, evidence suggests its occurrence from a few specific etiologies. Studies indicate a link between RDD and certain viral infections, including herpes simplex, Epstein-Barr, cytomegalovirus, and HIV. In addition, and as seen in this case, certain somatic mutations have been described in RDD; these include, but are not limited to, NRAS, KRAS, MAP2K1, and ARAF, genes that all play an important role in DNA synthesis and transcription processes [3]. Lastly, RDD has been shown to occur in approximately 10% of immunologic diseases, including systemic lupus erythematosus, idiopathic juvenile arthritis, and autoimmune hemolytic anemia [1].

Clinical Findings

RDD is a challenging diagnosis in pediatric patients due to its variable presentation and nonspecific symptoms. The classic RDD patient presents with bilateral massive, painless cervical lymphadenopathy with or without constitutional symptoms (i.e. fevers, night sweats, and weight loss) [4]. Symptoms and lesion growth typically progress gradually over the course of 3-6 months, a notable distinction from the acute onset described in this case. Other commonly involved lymph nodes include mediastinal, axillary, and inguinal. In approximately 43% of cases, RDD demonstrates extranodal spread to essentially any

other bodily organ which can cause a wide range of clinical manifestations. For instance, one case report described a 10-year-old male diagnosed with RDD of the pituitary sella who presented initially with symptoms of polyuria and polydipsia [5]. Another case described a 12-year-old male who presented with shortness of breath and chest pain later found to be due to an extranodal RDD cardiac mass along the interatrial septum [6]. Patients with RDD typically demonstrate leukocytosis, microcytic anemia, and elevated inflammatory markers, but lactate dehydrogenase (LDH) is normal; this distinguishes RDD from other malignancies, such as lymphoma, that present with an elevated LDH [7].

Although it is rare, RDD can be associated with other diseases leading to more serious complications. For instance, RDD with immunoglobulin G4-positive (IgG4+) plasma cells, termed IgG4-related RDD, can predispose a patient to AA amyloidosis leading to clinical features of kidney and liver failure [8]. Due to this concern for IgG4-related RDD, the Histiocyte Society recommends the IgG4/IgG ratio be evaluated in all patients diagnosed with RDD [9]. Neoplasia-associated RDD has also been documented in patients with Hodgkin and Non-Hodgkin lymphoma, cutaneous clear cell sarcoma, and myelodysplastic syndrome [1].

Imaging and Pathology Findings

Imaging plays an important role in guiding management of RDD. Chest x-ray and abdominal US are initially recommended for evaluation of pediatric patients, whereas CT scan of the neck, chest, abdomen and pelvis is the preferred work-up for adult patients, although FDG-PET/CT can also be utilized for initial staging and determining extranodal spread as RDD lesions are FDG-avid. Due to the radiation exposure associated with PET/CT and the preference to minimize this in pediatric patients, whole-body MRI is instead recommended for children [1]. However, downsides to whole-body MRI in pediatric patients is the requirement for patient sedation, which carries its own risks, as well as every medical center not having the capabilities to perform this imaging study. In situations where further imaging is required, this is best determined on a case-by-case basis dependent upon the patient's symptoms.

Due to the various phenotypes of RDD and the location in which it can present, the imaging findings tend to be patient-specific. In general, RDD presents with focal or multifocal masses/lymphadenopathy, which may be revealed on x-ray. If sufficiently large, the mass can displace nearby organs (i.e. bowel loops). RDD masses tend to be solid and hypoechoic on sonography. On CT, RDD masses are well-defined and enhance following contrast administration. Parenchymal edema may be seen if the mass is large enough to involve surrounding structures. On MRI, RDD lesions are isointense on T1- and hypointense on T2-weighted imaging, and homogeneously enhancing following gadolinium administration. RDD lesions are FDG-avid, demonstrating increased radiotracer uptake on PET/CT [10].

Biopsy with histological and immunohistochemical analysis is required to establish a final diagnosis of RDD. The immunophenotype of RDD is positive for CD68, OCT2, S100, and Cyclin D1 and negative for CD1a, as seen in this case [11]. In contrast, Langerhans-cell histiocytosis is positive for CD1a and Erdheim-Chester disease is negative for S100 [1]. Furthermore, RDD demonstrates an emperipolesis pattern on histology, which is caused by lymphocytes engulfing large, pale histiocytic cells. Conversely, Erdheim-Chester disease classically shows an xanthomatous appearance with Touton giant cells [12].

Treatment & Prognosis

Pediatric patients with RDD tend to have a favorable prognosis with treatment typically geared towards symptom control. Although literature provides insufficient data on the survival rate for RDD in pediatric patients, it is well-documented that those with nodal and cutaneous disease tend to have better outcomes and a more predictable clinical course. On the contrary, multifocal and extranodal RDD involving the spine, kidneys, liver, or lower respiratory tract tend to have an unfavorable prognosis [1]. Gain-of-functions mutations of the MAPK pathway, such as the *KRAS* mutation seen in our case, are also associated with RDD but it is unclear how these mutations affect patient morbidity [13].

In most cases of RDD, observation with routine follow-up is sufficient as 20-50% of patients will have spontaneous remission. In symptomatic cases, oral steroid therapy is useful in reducing mass size with the literature supporting it as an effective first-line treatment [14]. In cases refractory to steroids, other therapies such as immunotherapy, chemotherapy, and surgical debulking can be explored on a case-by-case basis. Immunomodulatory agents and monoclonal antibodies have shown efficacy in treating patients with refractory RDD. For instance, Thalidomide is a type of antiangiogenic drug which works by targeting interleukin-6 (IL-6), a pro-inflammatory cytokine implicated in the pathogenesis of RDD and other malignancies [15]. RDD has demonstrated a variable response to Thalidomide with the most successful treatments occurring in patients with the cutaneous form of RDD [1,16]. Furthermore, Rituximab and Siltuximab are monoclonal antibodies against CD20 and IL-6, respectively, which have shown efficacy in treating disseminated and immune-related RDD cases [17,18].

Chemotherapy is another adjunct therapy for treating pediatric patients with RDD. These drugs include purine analogs (i.e. cladribine), folate antagonists (i.e. methotrexate), and vinca alkaloids (i.e. vinblastine). One drug regimen in particular which was successful in curing a 12.5-year-old female with RDD included prednisone, 6-mercaptopurine, methotrexate, and vinblastine [1,19].

Targeted chemotherapy with mitogen-activated protein kinase (MEK) inhibitors can be utilized in cases of RDD with known mutations involving the MAPK pathway [1]. The *KRAS* mutation, as seen in our case, has been implemented in

RDD and has become a promising drug target. Cobimetinib, a MEK inhibitor currently used to treat *BRAF* V600K metastatic melanoma, was recently granted FDA approval for the treatment of histiocytic neoplasms in adults following a phase II clinical trial (NCT02649972) [20]. To date, multiple studies and case reports have shown Cobimetinib to be efficacious in treating RDD with an activating mutation in codon 12 of *KRAS* (p.G12R) [13]. Despite this promising advancement in adults, Cobimetinib is not currently FDA approved for use in pediatric patients.

Lastly, surgical resection is best utilized to treat unifocal RDD as well as symptomatic cases involving the spine and airway. Case series with surgical resection have demonstrated long-term remission of isolated cutaneous and intracranial disease [1].

Based on the literature, is unclear what constitutes the best short- and long-term approach to treating pediatric patients with RDD. After the initiation oral steroid therapy, adjunct therapy is best implemented on a case-by-case basis accounting for associated diseases, extranodal involvement, and the potential side effect profile.

Differential Diagnosis

The differential diagnosis for pediatric patients presenting with an inguinal swelling include a hernia, mass, and in males specifically, a hydrocele of the spermatic cord or testicular torsion [21]. Appendicitis can also present as an inguinal swelling when the inflamed appendix gets entrapped within a protruded hernial sac, termed an Amyand's hernia [22]. Masses include benign causes such as a lipoma, hematoma, or dermoid cyst as well as malignant causes such as a soft tissue sarcoma or lymphoma. Following a thorough history and physical examination, US with doppler is the most useful diagnostic tool for establishing an initial cause for the inguinal swelling [21]. In this case, US demonstrated a soft tissue mass with surrounding lymphadenopathy and ruled out a bowel-containing hernia or torsion.

Pediatric patients presenting with clinical features of RDD require an extensive work-up initially as a result of the broad differential diagnosis an inguinal soft tissue mass generates. Clinical management is further complicated by the disease's non-specific findings and potential to involve any organ system. Although RDD strongly mimics malignancy (i.e. non-Hodgkin lymphoma), other differential diagnoses include Langerhans cell histiocytosis, Erdheim-Chester disease, reactive lymphadenopathy, or in coexistence with an autoimmune disorder. A comparison of these diagnoses can be found in (Table 2) of the appendix.

Non-Hodgkin Lymphoma

Like RDD, non-Hodgkin lymphoma (NHL) can have a wide spectrum of phenotypical presentations depending on organ involvement. Patients with NHL typically present with

fever, weight loss, night sweats, and painless lymphadenopathy. In patients with gastrointestinal tract involvement, they may complain of epigastric pain, anorexia, and nausea [23]. Radiographs may reveal bowel wall thickening and displacement secondary to intra-abdominal masses. Bowel wall thickening and loss of stratification may also be seen on US, in addition to hypoechoic and hypo-vascular intra-abdominal masses/lymphadenopathy with loss of the normal echogenic hilum [24]. Masses/lymphadenopathy are hypo-attenuating with minimal contrast enhancement on CT, a key distinguishing feature compared to the hyperattenuating masses seen in RDD. On both T1- and T2-weighted MR imaging, masses appear hypointense with mild heterogeneous enhancement following gadolinium administration and restricted diffusion. PET/CT typically reveals focal or multifocal bone marrow infiltration [25].

Reactive Lymphadenopathy

Reactive lymphadenopathy is a benign disorder in which lymph nodes swell, most commonly in response to infection. In patients without signs of infection, it's important to distinguish this entity from more ominous conditions such as RDD. Reactive lymph nodes may be normal in size and are typically only visible on x-ray if markedly enlarged. Reactive lymph nodes demonstrate increased cortical echogenicity and loss of the echogenic hilum on US, with increase in peripheral vascularity on Doppler imaging [26]. Reactive lymph nodes demonstrate central fluid attenuation, if suppurative, with irregular peripheral enhancement and surrounding inflammatory changes on CT and are enlarged and hypertense on both T1- and T2-weighted MRI (allowing for differentiation from RDD). Following gadolinium administration, reactive lymphadenopathy is heterogeneously-enhancing; and, similar to other modalities, loss of the fatty hilum is observed. Similar to RDD, there is increased radiotracer uptake in reactive lymphadenopathy on PET/CT [27].

Erdheim-Chester Disease

Erdheim-Chester Disease (ECD) is a type of non-Langerhans histiocytosis which primarily involves the long bones. Patients typically present with bone pain originating from the legs and arms, joint pain, and muscle pain. If left untreated, ECD can lead to neurological symptoms including diabetes insipidus, exophthalmos, cerebellar ataxia, and panhypopituitarism [28]. Over half of the cases of ECD are associated with a mutation in the *BRAF* V600E gene, a unique etiology when compared to the other non-Langerhans cell histiocytic disorders [29]. As a slow-growing blood cancer, ECD manifests insidiously with multifocal and often symmetric sclerotic lesions of the metaphyses and diaphyses of the involved bones, which can be seen on radiographs [30]. Due to its predominantly osseous involvement, US is not commonly utilized to diagnose ECD. CT may reveal characteristic "hairy kidneys," encasement of the kidneys with hypo-attenuated, homogenous soft tissue with spiculated contours. On T1- and T2-weighted MRI, pathologic tissue is isointense to skeletal muscle, with minimal homogenous

contrast enhancement. On 99m-Tc bone scan, there is symmetric, bilateral uptake in the involved bones which spares the epiphyseal region [31]. ECD is reliably distinguished from RDD based on imaging findings and via histochemical analysis: while RDD is positive for S100 staining, ECD is negative [1].

Langerhans-Cell Histiocytosis

Langerhans-Cell Histiocytosis (LCH) results from abnormal proliferation of Langerhans cells, a type of antigen-presenting dendritic cell which resides in the epithelia of the skin. LCH is typically asymptomatic in children. When symptoms are present, the most frequent presenting signs include bone pain and a seborrheic rash [32]. Radiographs demonstrate solitary or multiple punched-out osseous lesions without a sclerotic rim. On US, LCH lesions are solid and hypoechoic, with minimal vascularity. On CT, LCH lesions are well-defined and hypoattenuating with cortical erosion and soft tissue involvement. On MRI, LCH lesions are hypointense to isointense on T1- and hyperintense on T2-weighted imaging, and they diffusely and homogeneously enhance following gadolinium administration [33]. PET/CT is not routinely used to diagnose LCH as the observed changes in radiotracer uptake are nonspecific. As previously noted, histochemical analysis is key in distinguishing between RDD and LCH: while LCH is positive on CD1a staining, RDD is negative [1].

CONCLUSION

In conclusion, this is a unique, challenging clinical case of RDD and, to the best of our knowledge, the first reported case of RDD involving the inguinal region in an infant under 1 year of age. Due to its rarity, there are still many uncertainties surrounding the pathogenesis, radiographical findings, and treatment plan for these patients. It is therefore crucial for clinicians to supplement radiology findings with other valuable clinical tools, such as pathology findings, histochemical analyses, and laboratory tests. In most cases, and in part due to the lack of literature on managing patients with RDD, organizing multidisciplinary provider meetings can be particularly effective for ensuring optimal and consistent care.

TEACHING POINT

Rosai-Dorfman Disease (RDD) is a difficult pediatric diagnosis due to its variable presentation and nonspecific radiologic findings which can lead to misguided management and unnecessary procedures. Paired with pathology and histochemical analysis, MRI with contrast is the mainstay imaging technique for diagnosing RDD in pediatric patients with a mass and surrounding lymphadenopathy demonstrating avid, homogenous enhancement.

AUTHORS' CONTRIBUTIONS

Thomas Hartmann, B.S.: Authored contributed to the writing of the manuscript, gathering radiographical images, and editing of the final case report.

Nadia Solomon, MD, MSc, MA: Authored contributed to the writing of the manuscript, gathering radiographical images, and editing of the final case report.

Gabriel Lerner, MD, MS: Authored contributed to the writing of the manuscript, gathering pathology images, and editing of the final case report.

Lauren Ehrlich, MD: Authored contributed to the writing of the manuscript, gathering radiographical images, and editing of the final case report.

Published Statement of Informed Consent

Did the author obtain written informed consent from the patient for submission of this manuscript for publication? (Answer with yes or no.)

No.

Human and animal rights

Not applicable.

Keywords: *Rosai-Dorfman Disease; Sinus histiocytosis with massive lymphadenopathy; Inguinal Pediatric; Magnetic Resonance Imaging, Ultrasound*

QUESTIONS

1. What is an alternative name for Rosai-Dorfman Disease?
 1) Histiocytic Sarcoma
 2) Sinus Histiocytosis with Massive Lymphadenopathy (applies)

- 3) Tuberculous Adenopathy
 4) Idiopathic Multicentric Lymphadenopathy
 5) Reactive lymphadenopathy

Explanation:

1) This name refers to a rare non-Langerhans histiocyte disorder involving cells of the hematopoietic lineage.

2) This is an alternative name for Rosai-Dorfman Disease. [Rosai-Dorfman Disease, also called sinus histiocytosis with massive lymphadenopathy, occurs due to an overproduction of histiocytes in the lymph nodes.]

3) This term describes the enlarged lymph nodes caused by tuberculosis, not Rosai-Dorfman Disease.

4) This is another name for Castleman Disease, a group of lymphoproliferative disorders characterized by lymph node enlargement.

5) This term describes enlarged lymph nodes which may be seen in the setting of infectious or inflammatory conditions.

2. What is the first line imaging technique recommended in pediatric patients with suspected Rosai-Dorfman Disease? Select the best answer.

- 1) CT scan of the neck, chest, abdomen and pelvis
 2) Abdominal Ultrasound
 3) MRI of the abdomen

- 4) Abdominal Ultrasound and Chest X-Ray (applies)
- 5) FDG-PET/CT

Explanation:

1) CT scan of the neck, chest, abdomen, and pelvis is the recommended imaging study for initial assessment of adult patients, not pediatric.

2) Abdominal ultrasound is one of the first line imaging techniques used to assess pediatric patients with RDD. Of note, a chest x-ray is warranted as well.

3) While MRI of the abdomen is not recommended as a first line imaging study in pediatric patients with RDD, it can be a helpful supplemental study.

4) The combination of abdominal ultrasound with chest x-ray is considered first line in the imaging investigation of pediatric patients with suspected RDD. [A chest x-ray and abdominal ultrasound are initially recommended for pediatric patients.]

5) FDG-PET/CT is a useful staging technique for patients with confirmed RDD, however it is not recommended as the first-line imaging technique for diagnosing RDD in pediatric patients.

3. Which of the following can be used to treat pediatric patients with Rosai-Dorfman Disease?

- 1) Oral Steroid Therapy
- 2) Chemotherapy
- 3) Immunotherapy
- 4) Surgical Debulking
- 5) All the above (applies)

Explanation:

1) Oral steroid therapy is commonly used to treat pediatric patients with Rosai-Dorfman Disease, especially to decrease symptoms secondary to mass effect.

2) Chemotherapy can be used to treat pediatric patients with Rosai-Dorfman Disease, especially if they are refractory to oral steroid therapy.

3) Immunotherapy can be used to treat pediatric patients with Rosai-Dorfman Disease, especially if they are refractory to oral steroid therapy.

4) This surgical technique can be used to treat pediatric patients with Rosai-Dorfman Disease, especially if they are refractory to steroids, chemotherapy, and immunotherapy.

5) All the listed therapies are treatment options for pediatric patients with Rosai-Dorfman Disease. [In symptomatic cases, oral steroid therapy is useful in reducing mass size with the literature supporting it as an effective first-line treatment. In cases refractory to steroids, other therapies such as immunotherapy, chemotherapy, and surgical debulking can be explored on a case-by-case basis.]

4. Which of the following answer choices is false?

1) The pathogenesis of Rosai-Dorfman Disease is poorly defined with accepted theories including a viral or genetic etiology

2) Most cases (20-50%) of Rosai-Dorfman Disease resolve spontaneously without treatment

3) The average age of onset of Rosai-Dorfman Disease is 1.5 years of age (applies)

4) Extranodal Rosai-Dorfman Disease involving the kidney, liver, or lower respiratory tract tends to have an unfavorable prognosis

5) Rosai-Dorfman Disease shows an increased FDG tracer uptake on PET/CT

Explanation:

1) This is a true statement. The pathogenesis of Rosai-Dorfman Disease is poorly defined with accepted theories including a viral or genetic etiology. In addition, RDD has been associated with immunodeficiency disorders including systemic lupus erythematosus and idiopathic juvenile arthritis

2) This is a true statement. 20-50% of Rosai-Dorfman Disease cases resolve spontaneously without treatment.

3) This statement is false. The average of onset of Rosai-Dorfman Disease is 20.6 years of age. [The disease prevalence is higher in males than females (58% to 42%) with a mean age of onset of 20.6 years.]

4) This is a true statement. Extranodal Rosai-Dorfman Disease tends to have an unfavorable prognosis. Due to this, more aggressive treatment is recommended earlier compared to the focal or cutaneous forms of RDD.

5) This is a true statement. PET/CT can be used to for initial staging and diagnosing extranodal spread in patients with RDD since it is FDG-avid.

5. Which of the following lab values is NOT associated with Rosai-Dorfman Disease? Select the best answer.

- 1) Elevated erythrocyte sedimentation rate
- 2) Low mean corpuscular volume
- 3) Elevated neutrophils
- 4) Elevated lactate dehydrogenase (applies)
- 5) Elevated C-reactive protein

Explanation:

1) This is a true statement. Erythrocyte sedimentation rate (ESR) is commonly elevated in patients with Rosai-Dorfman Disease, which is consistent the inflammatory nature of the disease.

2) This is a true statement. Rosai-Dorfman Disease commonly presents with lab values consistent with microcytic anemia (low mean corpuscular volume).

3) This is a true statement. Rosai-Dorfman Disease commonly presents with leukocytosis (elevated neutrophils), which can make it difficult for clinicians to distinguish the disease from an infectious etiology based on labs.

4) This is a false statement. Elevated lactate dehydrogenase (LDH) is more characteristic of non-Hodgkin's lymphoma, a common differential diagnosis in patient's with Rosai-Dorfman Disease. RDD commonly presents with normal LDH. [In addition, RDD presents with a normal lactate dehydrogenase (LDH), a key distinguishing factor from other malignancies, such as lymphoma, that present with an elevated LDH.]

This is a true statement. Similar to ESR, C-reactive protein levels are elevated in Rosai-Dorfman Disease which is consistent with the inflammatory nature of the disease.

REFERENCES

1. Abla O, Jacobsen E, Picarsic J, et al. Consensus recommendations for the diagnosis and clinical management of Rosai-Dorfman-Destombes disease. *Blood*. 2018; 131(26): 2877-2890. PMID: 29720485.
2. Patel MH, Jambhekar KR, Pandey T, Ram R. A rare case of extra nodal Rosai-Dorfman disease with isolated multifocal osseous manifestation. *Indian J Radiol Imaging*. 2015; 25(3): 284-287. PMID: 26288524.
3. Garces S, Medeiros LJ, Patel KP, et al. Mutually exclusive recurrent KRAS and MAP2K1 mutations in Rosai-Dorfman disease. *Mod Pathol*. 2017; 30(10): 1367-1377. PMID: 28664935.
4. Xu Y, Han B, Yang J, Ma J, Chen J, Wang Z. Soft tissue Rosai-Dorfman disease in child: A case report and literature review. *Medicine (Baltimore)*. 2016; 95(29): e4021. PMID: 27442634.
5. Zhang Y, Liu J, Zhu J, et al. Case Report: Rosai-Dorfman Disease Involving Sellar Region in a Pediatric Patient: A Case Report and Systematic Review of Literature. *Front Med (Lausanne)*. 2020; 7:613756. PMID: 33330575.
6. Yontz L, Franco A, Sharma S, Lewis K, McDonough C. A case of Rosai-Dorfman disease in a pediatric patient with cardiac involvement. *J Radiol Case Rep*. 2012; 6(1): 1-8. PMID: 22690274.
7. Yadav C, et al. Serum Lactate Dehydrogenase in Non-Hodgkin's Lymphoma: A Prognostic Indicator. *Indian J Clin Biochem*. 2016; 31(2): 240-242.
8. Röcken C, Wieker K, Grote HJ, Müller G, Franke A, Roessner A. Rosai-Dorfman disease and generalized AA amyloidosis: a case report. 2000; *Hum Pathol*. 31(5): 621-624. PMID: 10836304.
9. Emile JF, Abla O, Fraitag S, et al. Revised classification of histiocytoses and neoplasms of the macrophage-dendritic cell lineages. *Blood*. 2016; 127(22): 2672-2681. PMID: 26966089.
10. Weerakkody Y, Worsley C. Rosai-Dorfman Disease. *Radiopaedia*. 2022.
11. Ravindran A, Goyal G, Go RS, Rech KL. Rosai-Dorfman Disease Displays a Unique Monocyte-Macrophage Phenotype Characterized by Expression of OCT2. *Am J Surg Pathol*. 2021; 45(1): 35-44. PMID: 33177341.
12. Ozkaya N, Rosenblum MK, Durham BH, et al. The histopathology of Erdheim-Chester disease: a comprehensive review of a molecularly characterized cohort. *Modern Pathology*. 2018; 31(4): 581-597. PMID: 29192649.
13. Jacobsen E, Shanmugam V, Jagannathan J. Rosai-Dorfman Disease with Activating KRAS Mutation — Response to Cobimetinib. *N Engl J Med*. 2017; 377(24): 2398-2399. PMID: 29236635.
14. di Dio F, Mariotti I, Coccolini E, Bruzzi P, Predieri B, Iughetti L. Unusual presentation of Rosai-Dorfman disease in a 14-month-old Italian child: a case report and review of the literature. *BMC Pediatr*. 2016; 16: 62. PMID: 27142277.
15. Elbaz Younes I, Sokol L, Zhang L. Rosai-Dorfman Disease between Proliferation and Neoplasia. *Cancers (Basel)*. 14(21): 5271. PMID: 36358690.
16. Li X, Hong Y, An Q, et al. Successful Treatment of Rosai-Dorfman Disease With Low-Dose Oral Thalidomide. *JAMA Dermatol*. 2013; 149(8): 992-993. PMID: 23783880.
17. Alqanatish JT, Houghton K, Bond M, Senger C, Tucker LB. Rituximab Treatment in a Child with Rosai-Dorfman Disease and Systemic Lupus Erythematosus. *J Rheumatol*. 2010; 37(8): 1783-1784. PMID: 20675857.
18. Lee H, King G, Garg K, Pan Z, Tobin J, Robinson WA. Successful treatment of disseminated Rosai-Dorfman disease with siltuximab. *Haematologica*. 2018; 103(7): e325-e328. PMID: 29599203.
19. Jabali Y, Smrcka V, Pradna J. Rosai-Dorfman disease: successful long-term results by combination chemotherapy with prednisone, 6-mercaptopurine, methotrexate, and vinblastine: a case report. *Int J Surg Pathol*. 2005; 13(3): 285-289. PMID: 16086087.
20. Diamond EL, Durham BH, Ulaner GA, et al. Efficacy of MEK inhibition in patients with histiocytic neoplasms. *Nature*. 2019; 567(7749): 521-524. PMID: 30867592.
21. Mathison D. Evaluation of inguinal swelling in children. *UpToDate*. 2023;
22. Ivanschuk G, Cesmebasi A, Sorenson EP, Blaak C, Loukas M, Tubbs SR. Amyand's hernia: a review. *Med Sci Monit*. 2014; 20: 140-146.
23. Sapkota S, Shaikh H. Non-Hodgkin Lymphoma. *StatPearls*. 2022;
24. Toma P, Granata C, Rossi A, Garaventa A. Multimodality Imaging of Hodgkin Disease and Non-Hodgkin Lymphomas in Children. *RadioGraphics*. 2007; 27(5): 1335-1354. PMID: 17848695.
25. Marie E, Navallas M, Katz DS, et al. Non-Hodgkin Lymphoma Imaging Spectrum in Children, Adolescents, and Young Adults. *RadioGraphics*. 2022; 42(4): 1214-1238. PMID: 35714040.
26. Pattanayak S, Chatterjee S, Ravikumar R, Nijhawan VS, Vivek Sharma, Debnath J. Ultrasound evaluation of cervical lymphadenopathy: Can it reduce the need of histopathology/cytopathology?. *Med J Armed Forces India*. 2018; 74(3): 227-234. PMID: 30093765.
27. Zhang F, Zhu L, Huang X, Niu G, Chen X. Differentiation of reactive and tumor metastatic lymph nodes with diffusion-weighted and SPIO-enhanced MRI. *Mol Imaging Biol*. 2013; 15(1): 40-47. PMID: 22588595.

28. Mazor RD, Manevich-Mazor M, Shoenfeld Y. Erdheim-Chester Disease: a comprehensive review of the literature. *Orphanet J Rare Dis.* 2013; 8: 137. PMID: 24011030.
29. Haroche J, Charlotte F, Arnaud L, et al. High prevalence of BRAF V600E mutations in Erdheim-Chester disease but not in other non-Langerhans cell histiocytoses. *Blood.* 2012; 120(13): 2700-2703. PMID: 22879539.
30. Zaveri J, La Q, Yarmish G, Neuman J. More than Just Langerhans Cell Histiocytosis: A Radiologic Review of Histiocytic Disorders. *RadioGraphics.* 2014; 34(7): 2008-2024. PMID: 25384298.
31. Kumar P, Singh A, Gamanagatti S, Kumar S, Chandrashekhara SH. Imaging findings in Erdheim-Chester disease: what every radiologist needs to know. *Pol J Radiol.* 2018; 83: e54-e62. PMID: 30038679.
32. Tillotson CV, Anjum F, Patel BC. Langerhans Cell Histiocytosis. *StatPearls.* 2022;
33. Singh G, Anan R, Ibrahim D, et al. Langerhans cell histiocytosis (skeletal manifestations). *Radiopaedia.* 2022;

FIGURES

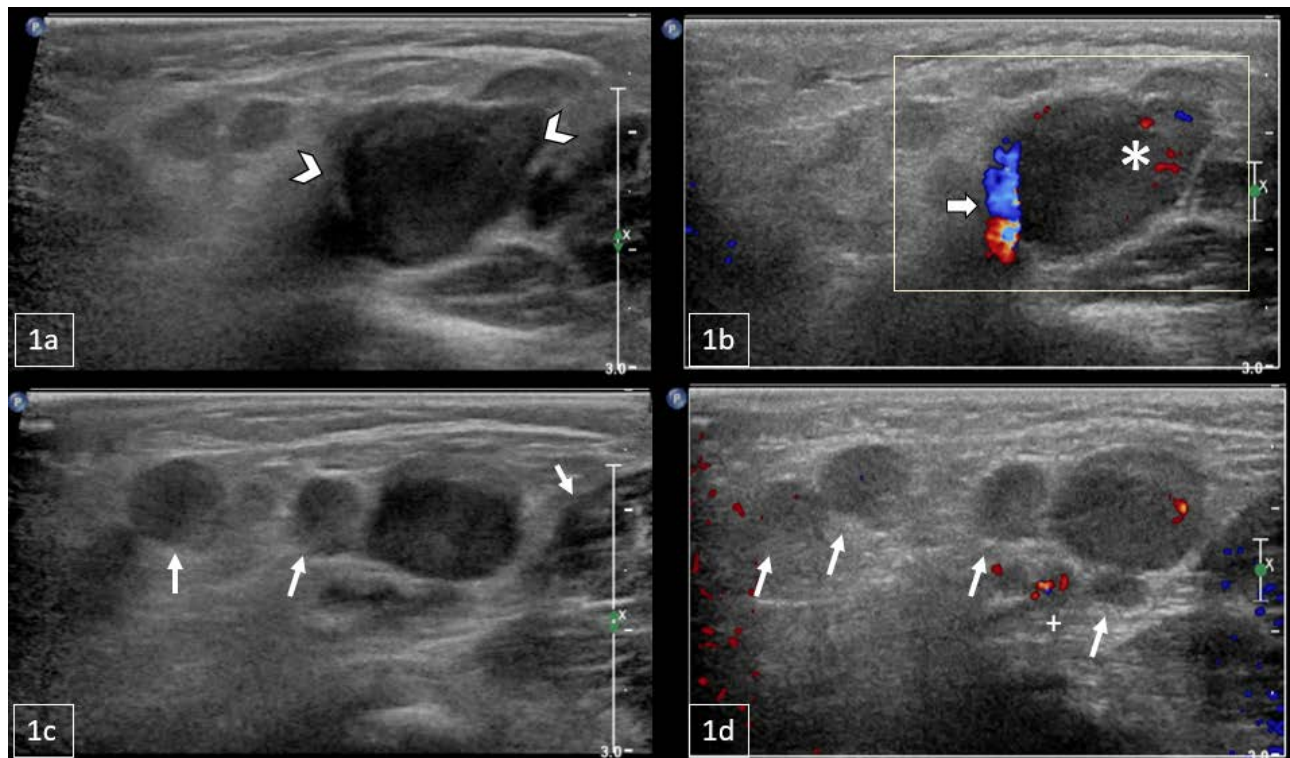


Figure 1: 11-month-old male with a palpable, reducible mass in the right inguinal region later diagnosed as Rosai-Dorfman Disease. FINDINGS: Sagittal US of the right inguinal canal: 1a) Grayscale US indicating a lobulated soft tissue mass extending into the right hemipelvis (arrowheads). 1b) Color Doppler US demonstrated the mass with internal vascularity (asterisk) with vessels along the rim surrounding the mass (arrow). 1c/d) Grayscale and Doppler US demonstrating multiple additional enlarged lymph nodes surrounding the mass of interest (arrows). TECHNIQUE: Sagittal grayscale (1a, 1c) and color Doppler US (1b, 1d) with a Philips 12-5 MHz linear array transducer.

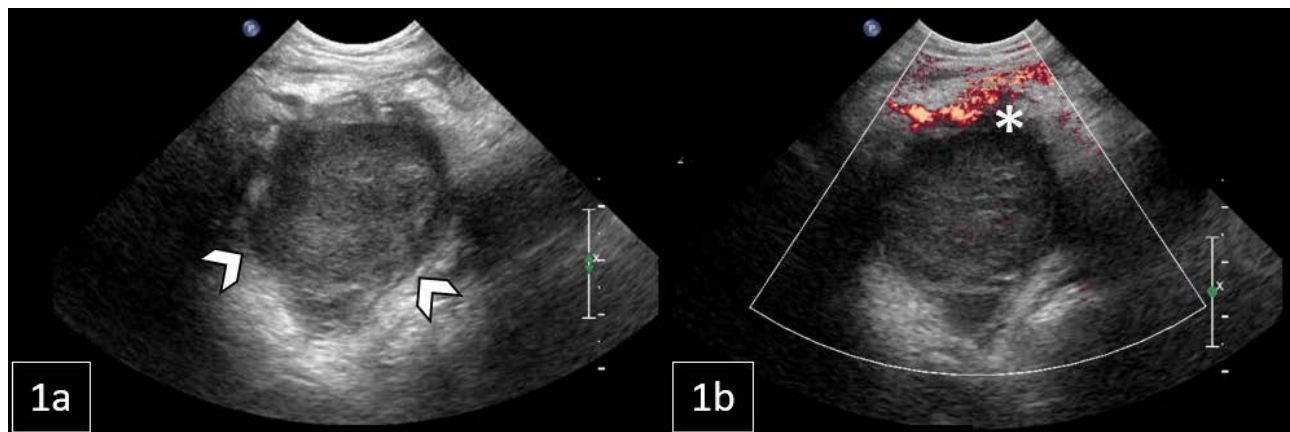


Figure 2: 11-month-old male with a palpable, reducible mass in the right inguinal region later diagnosed as Rosai-Dorfman Disease. FINDINGS: Right lower quadrant US: 1a) Grayscale US indicating a lobulated soft tissue mass extending into the right hemipelvis (arrowheads). 1b) Color Doppler US demonstrated vessels along the rim of the mass (asterisk). TECHNIQUE: Transverse grayscale (1a) and color Doppler US (1b) with a Philips 8-5 MHz curved array transducer.



Figure 3: 11-month-old male with a palpable, reducible mass in the right inguinal region later diagnosed as Rosai-Dorfman Disease. FINDINGS: MRI demonstrating a necrotic lesion at the posterior right pelvic inlet measuring 3.3cm (1a, axial) x 3.8cm (1b, coronal) x 4.3cm (1c, sagittal). Clustered lymphadenopathy extending along right external and common iliac region. TECHNIQUE: Pre-contrast HASTE (Half fourier Single-shot Turbo spin-Echo) 3T MRI.

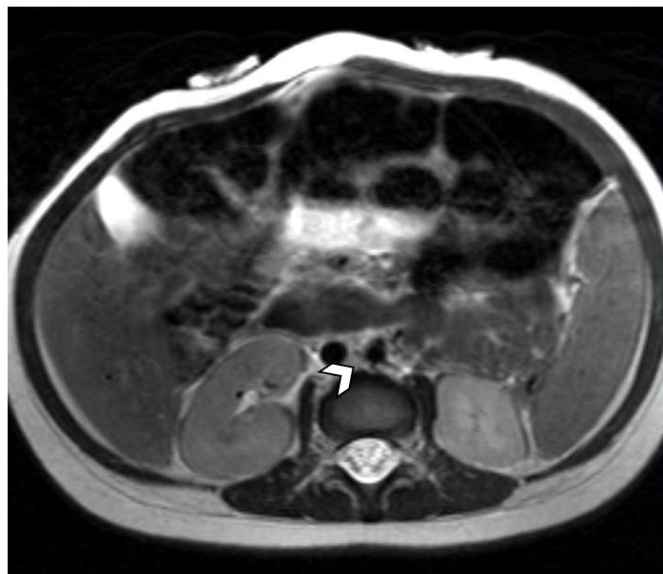


Figure 4: 11-month-old male with a palpable, reducible mass in the right inguinal region suspicious for malignancy. FINDINGS: MRI demonstrates a prominent lymph node in the interaortocaval area measuring 7.8mm. TECHNIQUE: Pre-contrast HASTE (Half fourier Single-shot Turbo spin-Echo) 3T MRI.



Figure 5: 11-month-old male with a palpable, reducible mass in the right inguinal region later diagnosed as Rosai-Dorfman Disease. FINDINGS: MRI demonstrates a prominent, hyper-enhancing lymph nodule in the left lateral chest wall measuring 10.9mm. TECHNIQUE: Post-contrast T1-weighted 3T MRI.

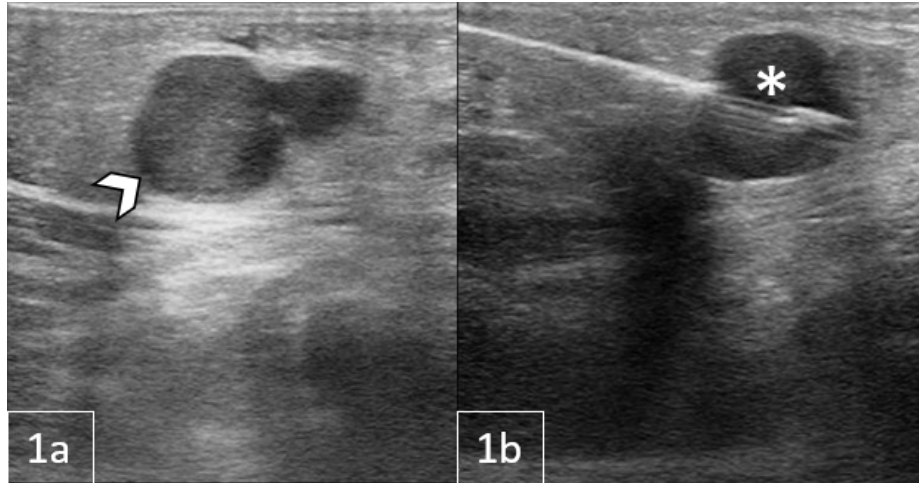


Figure 6: 11-month-old male with a palpable, reducible mass in the right inguinal region later diagnosed as Rosai-Dorfman Disease.
FINDINGS: 1a) Grayscale inguinal US demonstrating target mass prior to core needle biopsy. 1b) Needle in the transverse plane (asterisk) sampling the solid mass.
TECHNIQUE: Core-needle biopsy performed under US guidance in the transverse plane

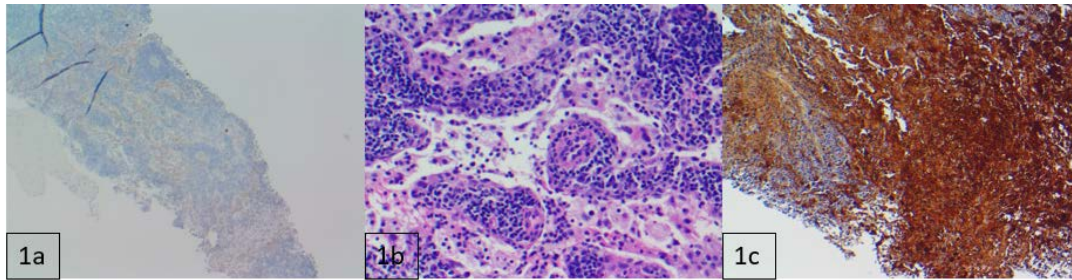


Figure 7: 11-month-old male with necrotic lesion at the pelvic inlet, posteriorly on the right, later diagnosed as Rosai-Dorfman Disease.
FINDINGS: Histochemical analysis following core needle biopsy: 1a) CD1a negative at 40x scale. 1b) Hematoxylin and eosin (H&E) stain demonstrating large pale histiocytes engulfing lymphocytes, consistent with emperipolesis. 1c) S100 positive at 100x scale.
TECHNIQUE: Pathologic evaluation of the mass following core-needle biopsy.

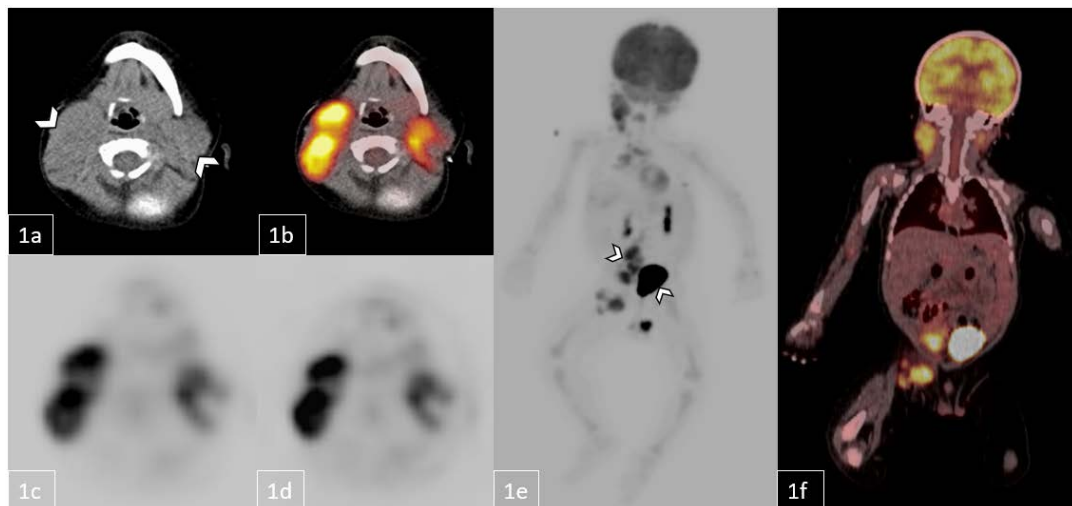


Figure 8: 11-month-old male with diagnosed Rosai-Dorfman Disease evaluated prior to starting therapy.
FINDINGS: Whole body PET-CT demonstrates multiple hypermetabolic conglomerate nodes within the right greater than left cervical, parotid, and supraclavicular areas, mediastinum, and left axillary regions (1a-d, white arrows). Abdomen and pelvis region show a large ill-defined hypermetabolic conglomerate mass extending from the aortocaval region to the lower pelvis, predominately on the right side, and multiple hypermetabolic nodes within the right inguinal region (1e/1f, white arrows).
TECHNIQUE: Whole Body Pet-CT: 1a) Low-dose non-contrast CT, 1b) Axial fused PET-CT, 1c) Axial PET attenuation corrected, 1d) Axial PET nonattenuation corrected, 1e) Coronal fused PET-CT, and 1f) Coronal PET Maximum Intensity Projection

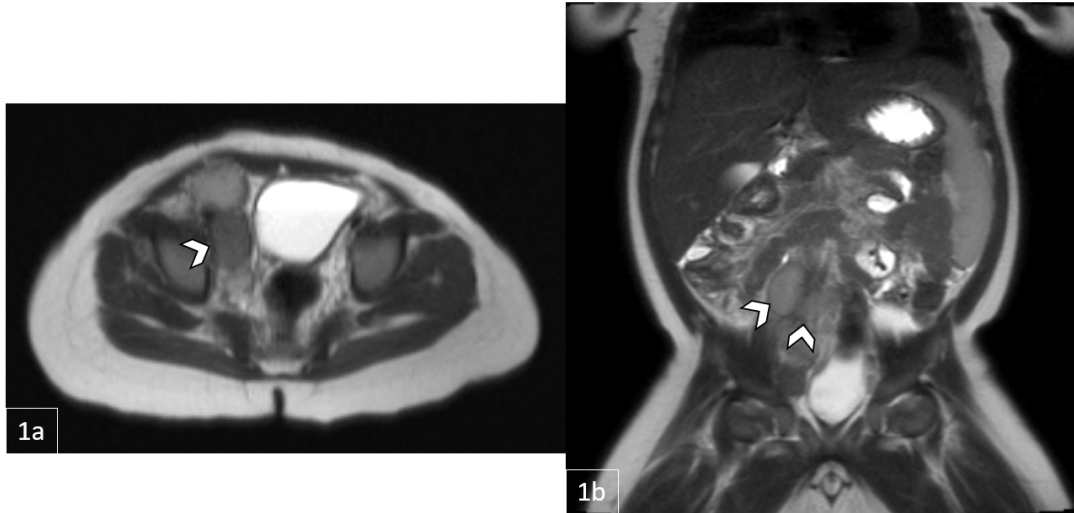


Figure 9: 11-month-old male with diagnosed Rosai-Dorfman Disease evaluated to assess response to oral prednisone therapy. FINDINGS: MRI demonstrates a lesion at the right pelvic inlet measuring 2.0cm in greatest diameter (1a/1b, white arrows). No significant changes in the surrounding clustered retroperitoneal and inguinal lymphadenopathy were identified when compared to prior. TECHNIQUE: Pre-contrast HASTE (Half fourier Single-shot Turbo spin-Echo) 3T MRI.



Figure 10: 11-month-old male with diagnosed Rosai-Dorfman Disease evaluated to assess response to oral prednisone therapy. FINDINGS: MRI demonstrates a mild interval decrease in diffuse lymphadenopathy involving the bilateral level Ib-XIII nodal stations throughout the neck and upper thorax. Representative nodes/nodal conglomerates include a 3.6 x 2.6 cm right nodal conglomerate, a left nodal mass posterior to the submandibular gland measuring 2.2 x 1.5 cm, and an additional right nodal mass measuring 1.1 x 0.7 cm (1a/1b, white arrows). A lymph node conglomerate is also visualized on the right measuring 4.4 x 2.5 cm (1c, asterisk). TECHNIQUE: Pre-contrast STIR (Short-TI Inversion Recovery) 3T MRI.

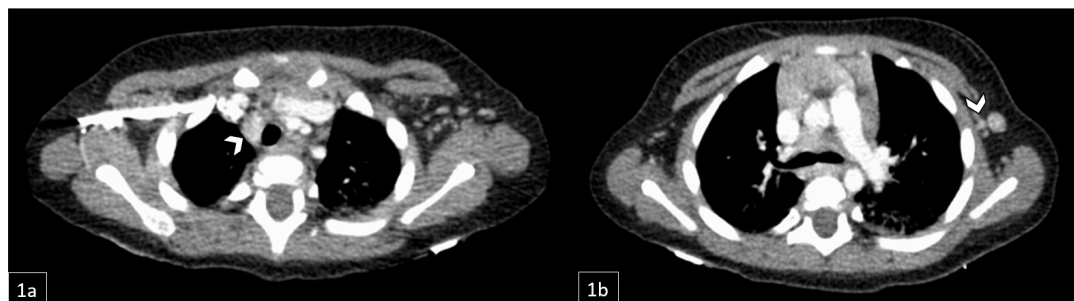


Figure 11: 11-month-old male with diagnosed Rosai-Dorfman Disease evaluated to assess response to oral prednisone therapy. FINDINGS: CT demonstrates right paratracheal lymphadenopathy, largest focus measuring about 1.5 x 1.1 cm (1a, white arrow). There is a left anterior chest wall nodule measuring approximately 0.7cm in the short axis (1b, white arrow), grossly stable since prior PET/CT. TECHNIQUE: Contrast-enhanced CT chest.

TABLES

Summary table: (Contains high yield information about the reported entity)

Etiology	Not well-defined; Theories include viral (HSV, CMV, HIV, and EBV), genetic (<i>NRAS</i> , <i>KRAS</i> , <i>MAP2K1</i> , and <i>ARAF</i> mutations), or in association with an autoimmune disorder
Incidence	100 cases per year in United States
Gender Ratio	Higher incidence in males vs females [58% to 42%]
Age Predilection	Mean age of onset is 20.6 years
Risk Factors	No risk factors have been identified
Treatment	Most cases do not require treatment; observation with close follow-up is typically sufficient Symptomatic control: - Oral steroid therapy - Alternatives: immunotherapy, chemotherapy, and surgical debulking on case-by-case basis
Prognosis	Dependent primarily on tumor site, extranodal involvement, and tumor size. Cases with most favorable prognosis include nodal and cutaneous forms of RDD. Multifocal and extranodal RDD, particularly those with kidney, liver, or lower respiratory tract disease, tend to have an unfavorable prognosis
Findings on Imaging	Variable due to disease spectrum; X-Ray = Appreciated as lymphadenopathy; CT = hyperattenuating and enhancing mass, parenchymal edema surrounding mass may be present; MRI = Isointense (T1), hypointense (T2), and homogenous enhancement (Gadolinium); Nuclear Medicine = Increased uptake on gallium scan and increased metabolism with FDG-PET

Table 1: Summary table of Rosai-Dorfman Disease.

Differential table: (Contains differential diagnoses of the reported entity)

	X-Ray	Ultrasound	CT	MRI	PET
Rosai-Dorfman Disease	Lymphadenopathy; if large, mass can displace nearby organs and bowel loops	Hypochoic, solid mass	Well-defined, hyperattenuating mass with peripheral contrast enhancement; +/- parenchymal edema	T1: isointense T2: hypointense T1 C+ (Gd): homogenous enhancement with restricted diffusion due to central necrosis	Increased FDG uptake
Non-Hodgkin Lymphoma (GI Tract)	Bowel wall thickening; bowel loop displacement by intra-abdominal masses	Hypochoic, hypovascular masses with bowel wall thickening and loss of stratification; enlarged lymph nodes with loss of echogenic hilum	Hypoattenuating masses with minimal enhancement; bowel wall thickening in a focal or diffuse distribution with enlarged lymph nodes surrounding vessels	T1: hypointense T2: hypointense T1 C+ (Gd): heterogeneously enhancing masses due to hypovascularity with restricted diffusion	FDG-avid masses with focal or multifocal bone marrow infiltration
Reactive Lymphadenopathy (i.e. Infection)	Lymphadenopathy (if sufficiently enlarged)	Increased cortical echogenicity with loss of echogenic hilum; peripheral vascularity on Doppler	Central fluid attenuation with irregular peripheral enhancement and surrounding inflammatory changes	T1: hyperintense T2: hyperintense T1 C+ (Gd): heterogeneously enhancing enlarged (>1cm) lymph nodes with loss of fatty hilum	Increased FDG uptake
Erdheim-Chester Disease	Lytic-sclerotic lesions of the metaphysis and diaphysis of the long bones	Not routinely utilized	Hypoattenuating, homogeneous masses with spiculated contours and weak contrast enhancement (i.e. characteristic “hairy kidneys”)	T1: isointense to muscle T2: isointense to muscle T1 C+ (Gd): minimal, homogeneous enhancement	Increased FDG uptake; 99mTc uptake in the long bones, typically symmetric, bilateral, and sparing the epiphyseal region
Langerhans-Cell Histiocytosis	Solitary or multiple punched out lytic lesions without sclerotic rim	Hypochoic, solid mass lesion with minimal vascularity	Well-defined, hypoattenuating osseous lesion with cortical erosion and soft tissue involvement	T1: hypointense to isointense T2: hyperintense T1 C+ (Gd): diffuse, homogeneous enhancement	Nonspecific; degree of radioactive tracer uptake dependent upon underlying disease

Table 2: Differential diagnosis table for Rosai-Dorfman Disease.

ABBREVIATIONS

RDD = Rosai-Dorfman Disease; NHL = Non-Hodgkin Lymphoma; CT = Computer Tomography; MRI = Magnetic Resonance Imaging; PET = Positron Electron Tomography; SUV = Standardized Uptake Value; EBV = Epstein-Barr virus; HIV = Human immunodeficiency virus; CMV = Cytomegalovirus; HSV = Herpes simplex virus; Gd = Gadolinium; FDG = Fluorodeoxyglucose

Online access

This publication is online available at:

www.radiologycases.com/index.php/radiologycases/article/view/4873

Peer discussion

Discuss this manuscript in our protected discussion forum at:

www.radiopolis.com/forums/JRCR

Interactivity

This publication is available as an interactive article with scroll, window/level, magnify and more features.

Available online at www.RadiologyCases.com

Published by EduRad



www.EduRad.org